Characterization and Application of Nanomaterials 2026, 9(3), 026250021.
https://doi.org/10.24294/can026250021

Article

Investigation of boehmite-modified castor oil-based nanofluid as a potential biolubricant

Surya Kumari Joshi[1,2,3,4,5], Dinesh Kumar Chaudhary[5,6], Md. Al-Mamun[5], Md. Saiful Islam[7], Md. Abdul Gafur[8], Aninda Nafis Ahmed[8], Surya Prasad Adhikari[9,*], Rabindra Prasad Dhakal[10,*], Sheikh Manjura Hoque[5,*], Rameshwar Adhikari[1,3,4,*]

[1] Central Department of Chemistry, Tribhuvan University, Kathmandu 44818, Kirtipur, Nepal
[2] Nepal Oil Corporation Limited, Tanka Prasad Ghumti Sadak, Kathmandu 44600, Babarmahal, Nepal
[3] Research Centre for Applied Science and Technology (RECAST), Tribhuvan University, Kathmandu 44618, Kirtipur, Nepal
[4] Nepal Polymer Institute (NPI), P. O. Box 24411, Kathmandu 44600, Kirtipur, Nepal
[5] Material Science Division, Atomic Energy Centre, 4, Kazi Nazrul Islam Avenue, Shahbagh, Dhaka-1000, Bangladesh
[6] Department of Physics, Amrit Campus, Tribhuvan University, Kathmandu 44600, Lekhnath Marg, Nepal
[7] Pharmaceutical Science Research Division, Bangladesh Council of Scientific and Industrial Research (BCSIR), Dhaka-1000, Bangladesh
[8] Pilot Plant and Process Development Center, Bangladesh Council of Scientific and Industrial Research (BCSIR), Dhaka-1000, Bangladesh
[9] Department of Mechanical and Aerospace Engineering, Pulchowk Campus, Tribhuvan University, Lalitpur 44700, Pulchowk, Nepal
[10] Nepal Academy of Science and Technology (NAST), Lalitpur 44700, Khumaltar, Nepal

*** Corresponding authors:** Surya Prasad Adhikari, surya@tcioe.edu.np; Rabindra Prasad Dhakal, rabindraprasaddhakal@gmail.com; Seikh Manjura Hoque, manjura_hoque@yahoo.com; Rameshwar Adhikari, nepalpolymer@yahoo.com

CITATION

Joshi S K, Chaudhary D K, Al-mamun M, et al. Investigation of boehmite-modified castor oil-based nanofluid as potential biolubricant. Characterization and Application of Nanomaterials. 2026; 9(3): 026250021. https://doi.org/10.24294/can026250021

ARTICLE INFO

Received: 18 June 2026
Accepted: 14 August 2026
Available online: 8 September 2026

Abstract: Nanofluids have recently captured the attention of researchers due to their numerous advantages, including improved cooling, lubricating, and thermal properties compared to pristine fluids. Producing a highly stable vegetable oil-based nanofluid with optimum kinematic viscosity is an important task for lubrication, which plays a crucial role in prolonging the lives of machines. This work investigates the stability, viscosity, and sustainability of castor nanofluid prepared by blending 0.1 wt.-% boehmite nanoparticles (B-NPs) under ultrasonication. The zeta potential of the nanofluid was measured to be −34.7 mV, indicating its good colloidal stability. The kinematic viscosity (KV) of castor oil was 49.81 ± 0.23, 25.38 ± 0.11, 14.77 ± 0.05, and 10.42 ± 0.02 cSt at 40 ± 0.5, 60 ± 0.5, 80 ± 0.5, and 100 ± 0.5 ℃, which was enhanced by approximately 27 cSt, 13 cSt, 5 cSt, and 4 cSt, respectively, upon the addition of the B-NPs at the corresponding temperatures. The KV values of both oil and nanofluid decreased with temperature. B-NPs have been demonstrated to be excellent viscosity modifiers, hence attesting to the castor oil-based nanofluid's potential suitability as a sustainable and eco-friendly lubricant as an alternative to petroleum-based ISO VG 68 hydraulic oil.

Keywords: nanoparticles; nanofluid; kinematic viscosity; zeta potential; lubrication

1. Introduction

The lubricant plays a crucial role in prolonging the lives of machines by reducing friction and wear, which ultimately leads to improved efficiency and lower maintenance costs. Keeping in mind their importance in industries, the investigation for improving the properties of lubricating oils has increased over the last few decades [1–3].

With the expansion of the petroleum industry in the 19th Century, petroleum-based lubricants were introduced and rapidly became significant, continuing to be widely utilized to this day. However, petroleum-based lubricants have been proven in many respects to be harmful to both humans and the environment [4,5]. To mitigate these risks, researchers have recently focused on developing vegetable oil-based nanofluids that are environmentally safe and exhibit outstanding lubricating properties with suitable viscosity, meeting the requirements of the machinery [6,7]. First, Choi, in 1995, proposed suspending metallic nanoparticles (NPs), like copper NPs, in heat transfer fluids such as water, engine oil, and ethylene glycol, and named them *nanofluids* at Argonne National Laboratory, USA. He reported higher thermal conductivity of the copper-water system nanofluids than that of their base fluids. Similarly, Eastman et al. (2001) found a significant enhancement in the thermal conductivity of the copper-ethylene glycol system nanofluid compared to pure ethylene glycol or ethylene glycol containing an equivalent volume fraction of suspended oxide NPs nanofluid [8,9]. Thereafter, the varieties of nanofluids have been developed for different engineering and biomedical applications, including lubrication, cooling, heat transfer, power generation, and machining [10–13] by dispersing the various NPs, such as magnesium oxide (MgO), graphene, hexagonal boron nitride (hBN), titania (TiO_2), copper oxide (CuO), cerium oxide (CeO_2), zinc oxide (ZnO), aluminium oxide (Al_2O_3), boehmite nanoparticles (B-NPs)

etc. [7,13–21]. For example, dispersion of MgO in H_2O significantly improves the thermal conductivity and heat transfer rate for cooling devices in biomedicine [13]. The dispersion of 1% hBN in castor oil minimized the coefficient of friction (COF) and wear by 30.2% and 51.7% at high load and low speed, respectively. The NPs were found to change the viscosity of castor oil on a massive scale [14]. Castor oil was also used for nanolubrication after blending with the surface-modified CuO. The COF and wear scar diameter (WSD) were minimized by 34.6% and 28.3% using this nanofluid in comparison to neat oil at optimum conditions [15]. In a similar way, CeO_2 and nanoscale polytetrafluoroethylene (PTFE) were used as nano-additives in castor oil to enhance anti-frictional as well as anti-wear behavior. The nanofluid containing 0.25% (w/v) CeO_2 showed the best anti-friction and anti-wear behavior. Additionally, the nanofluid containing 0.5 wt.-% and 0.1 wt.-% of PTFE particles was found to exhibit the best anti-friction and anti-wear performance, respectively [16].

The dispersion of a small amount of ZnO NPs in castor oil improved the anti-wear and extreme pressure qualities. Beyond that concentration, the nanofluid showed an increase in wear rate and also no significant improvement in the coefficient of friction (COF) [17].

Similarly, the dispersion of 0.2% TiO_2 NPs in castor oil lessened the COF in comparison to raw castor oil [18]. The castor oil exhibited excellent rheological and tribological properties after the addition of 30% sepiolite [19]. The dispersion of graphene nanoplatelets in castor oil moderately enhanced the viscosity of castor oil and improved the thermal conductivity, with exceptional heat transfer capacities for heat control applications [20].

The immersion of Al_2O_3 NPs in host transformer oil enhanced the insulation properties [21]. These reports clarify that the dispersion of NPs (sizes 1–100 nm) in base fluid improves the thermal characteristics, energy savings, rheological properties, and frictional characteristics of base fluid. This is due to the higher surface area of NPs.

Among the various NPs, boehmite NPs (B-NPs) represent a promising and economical addition due to their non-toxic characteristics, flame-retardant properties, and applicability across multiple domains such as coatings, catalysis, lubricants, ceramics, and electronics [22,23]. Some literature surveys related to B-NPs containing lubricants encourage extending the studies to investigate the castor oil-based nanofluids. For instance, the use of B-NPs dispersed in poly-α-olefins demonstrated superior performance in reducing friction, wear, and extreme pressure compared to the polymer alone [7]. The blending of B-NPs with jatropha oil resulted in a significant increase in kinematic viscosity (K.V.) of jatropha oil [24].

Additionally, castor oil nano-lubricants have been widely investigated and found to have outstanding lubricating properties, but not with a hydroxyl group-containing nanofiller. In view of the unique properties of the B-NPs (such as no toxicity, flame retardance, etc.) and their positive impact on the properties of other lubricants, a synergistic effect may be expected in the B-NP/castor oil combinations, which forms the motivation of this study.

In summary, in light of the available reports, the addition of NPs to the fluids increases the viscosity and thermal conductivity, thus improving the fluid's tribological behavior. The study to improve the properties of castor oil by dispersion of B-NPs has rarely been reported. Hence, this work reports the synthesis of castor nanofluid by dispersing a small amount of B-NPs and its characteristics towards its suitability for lubrication. Based on the literature reports so far, the present work is limited to 0.1 wt.-% of the B-NPs dispersed into the vegetable oil. The present work also presents the possible mechanism of modifying the flow properties of castor oil after dispersing B-NPs.

2. Experimental

2.1. Materials

Castor oil was purchased from Nike Chemical India, product code C-001140, and Batch No. 71116. The commercially available boehmite, AlO(OH), was obtained from Sasol in Hamburg, Germany, and is available as Dispersal OS1.

2.2. Preparation of castor nanofluid (CNF)

Castor nanofluid (CNF) was prepared by dispersing B-NPs in castor oil, following the procedure published previously [24]. In brief, castor nanofluid (CNF) was prepared by dispersing B-NPs in castor oil in two steps (see **Figure 1**). In the first step, 0.05 g B-NPs were homogenized into 49.95 g castor oil using a magnetic stirrer at a speed of 900 rpm at 60 ± 10 ℃ for 1 h. In the second step, the homogeneous solution thus obtained was ultrasonicated below 50 ℃ for 2 h, using a probe sonicator to form more uniformity. The nanofluid was characterized using different techniques like FTIR, zeta potential, K.V., viscosity index, etc. The B-NPs were further analyzed by X-ray diffractometer (XRD) and transmission electron microscope (TEM).

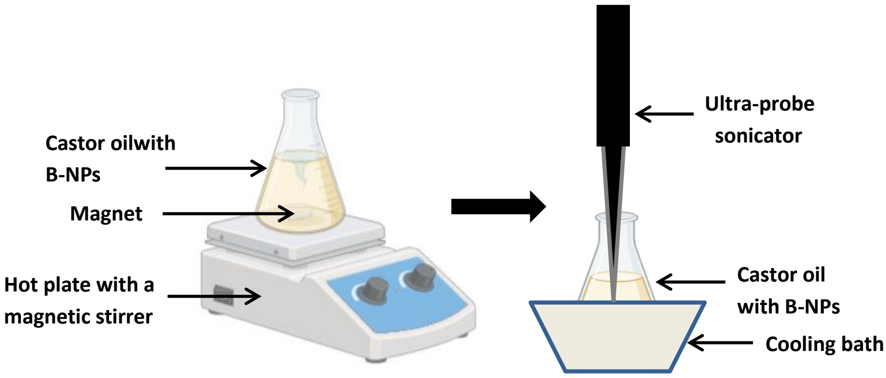

Figure 1. Schematic diagram showing the preparation of castor oil-based nanofluid.

2.3. Characterization techniques

X-ray Diffractometer (XRD): A fast-detector X-ray diffractometer (XRD) made in Japan by the Rigaku Corporation, Smart Lab, was utilized for the determination of the crystallite size of the B-NPs and phase analysis.

Transmission Electron Microscopy (TEM): The morphology of the NPs was analyzed by a high-resolution transmission electron microscope with energy-loss spectroscopy (TALOS F200 G2). The elemental components of the NPs were determined by energy-dispersive X-ray spectroscopy (EDX) (S50 QLD9111, FEI, Amsterdam, The Netherlands).

Nuclear Magnetic Resonance (NMR) Spectroscopy: The composition of castor oil was determined by proton nuclear magnetic resonance (^{1}H NMR), carbon nuclear magnetic resonance (^{13}C NMR), and distortionless enhancement by polarization transfer (DEPT-135) and was recorded by a Bruker Avance Neo 600 MHz NMR spectrometer. Deuterated chloroform ($CDCl_3$) was used as a solvent, and its chemical shift peak at 7.26 ppm was considered as an internal reference.

Zeta Potential Measurement: Zeta Sizer (Nano ZSUK, Malvern Instruments Limited) was used to determine the zeta potential of the nanofluid and the hydrodynamic diameter of B-NPs in the nanofluid.

Viscosity Measurement: The U-tube viscometer with a water bath was used to determine the kinematic viscosity (K.V.) at 40 ± 0.5, 60 ± 0.5, and 80 ± 0.5 ℃, and a silicon oil bath was used at 100 ± 0.5 ℃. Both water and silicon oil baths were used to measure the viscosity parameters (the K.V. and viscosity index, V.I. values) of the fluids. The presented values are an average of at least three measurements.

Pour Point and Cloud Point Estimation: A pour point and cloud point tester was used to measure the pour point of the oil and its nanofluid.

Fourier Transform Infrared (FTIR) Spectroscopy: FTIR (STA, 449 F3 Jupiter, UK) was used to analyze the functional groups.

3. Results and discussion

3.1. Characterization of boehmite nanoparticles (B-NPs)

The B-NPs, which appeared as a white powder, were characterized by XRD, TEM, EDS, and FTIR and reported in our previously published paper [24]. The XRD revealed the polycrystalline nature of B-NPs with a mean crystallite size of 8.2 nm. In the same way, the TEM and EDS showed that the B-NPs had a platelet structure with high purity, and the FTIR showed peaks of functional groups within the range of 3000–3600 cm^{-1} and 900–1100 cm^{-1}, as reported earlier [25–29]. All these properties of B-NPs are summarized in **Table 1.**

Table 1. Summary of physical properties of B-NPs investigated by different techniques.

Properties	**Details**	**Techniques used**
Average crystallite size	8.2 nm	XRD
Structure	Orthorhombic/Polycrystalline	XRD
Morphology	Nanoplatelet	TEM
Average grain size	11.8 nm	TEM
Elemental composition	Al and O	EDS

3.2. Characterization of castor oil (CO)

The terminal methyl protons are represented by the signal at δ_H 0.83 to 0.96 ppm in castor oil's proton nuclear magnetic resonance (^{1}H NMR). Similarly, long aliphatic methylene chains, β-carbonyl protons, allylic protons, α-methylene to ester, and bis-allylic protons are represented by the signals at δ_H 1.23 to 1.27 ppm, 1.58 to 1.98 ppm, 2.02 to 2.06 ppm, 2.26 to 2.32 ppm, and 2.73 to 2.77 ppm, respectively.

Furthermore, **Figure 2** illustrates the existence of olefinic protons at δ_H 5.23 to 5.35 ppm and a glycerol backbone at δ_H 4.10 to 4.28 ppm, respectively [30].

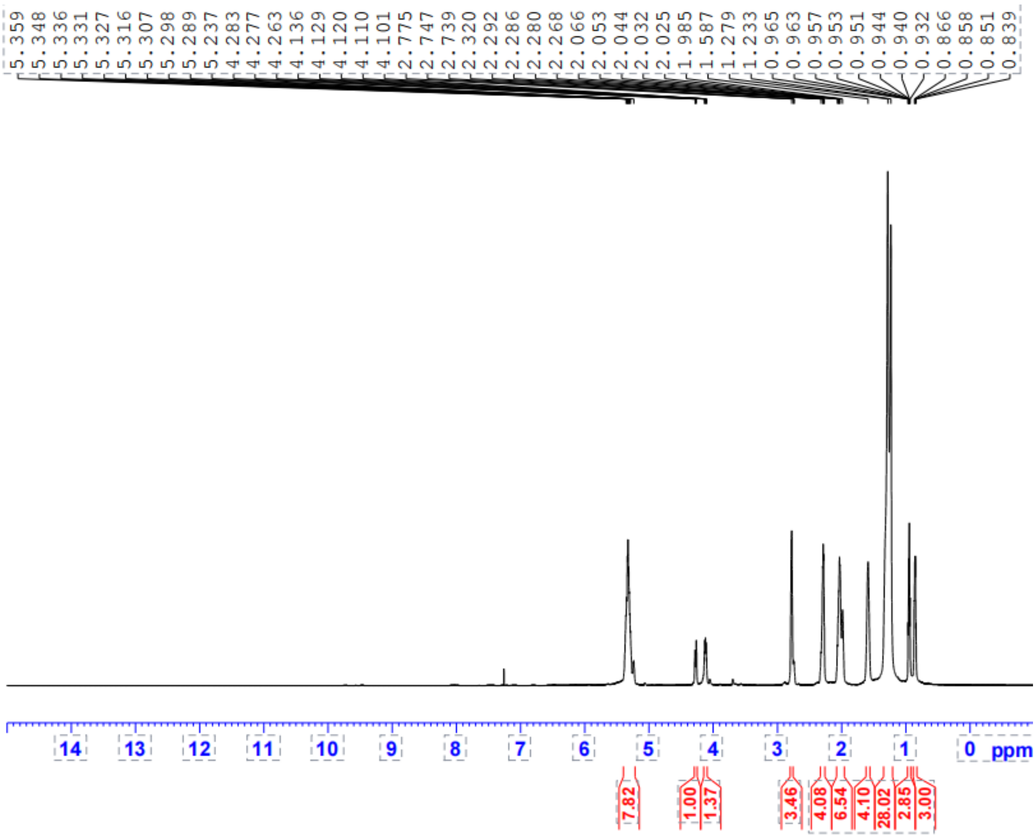

Figure 2. Proton nuclear magnetic resonance (1H NMR) spectrum of castor oil.

Furthermore, carbon-13 nuclear magnetic resonance (^{13}C NMR) and distortionless enhancement by polarization transfer (DEPT-135) were performed for the structure elucidation of castor oil (CO), and the results are presented in **Figures 3** and **4**, respectively.

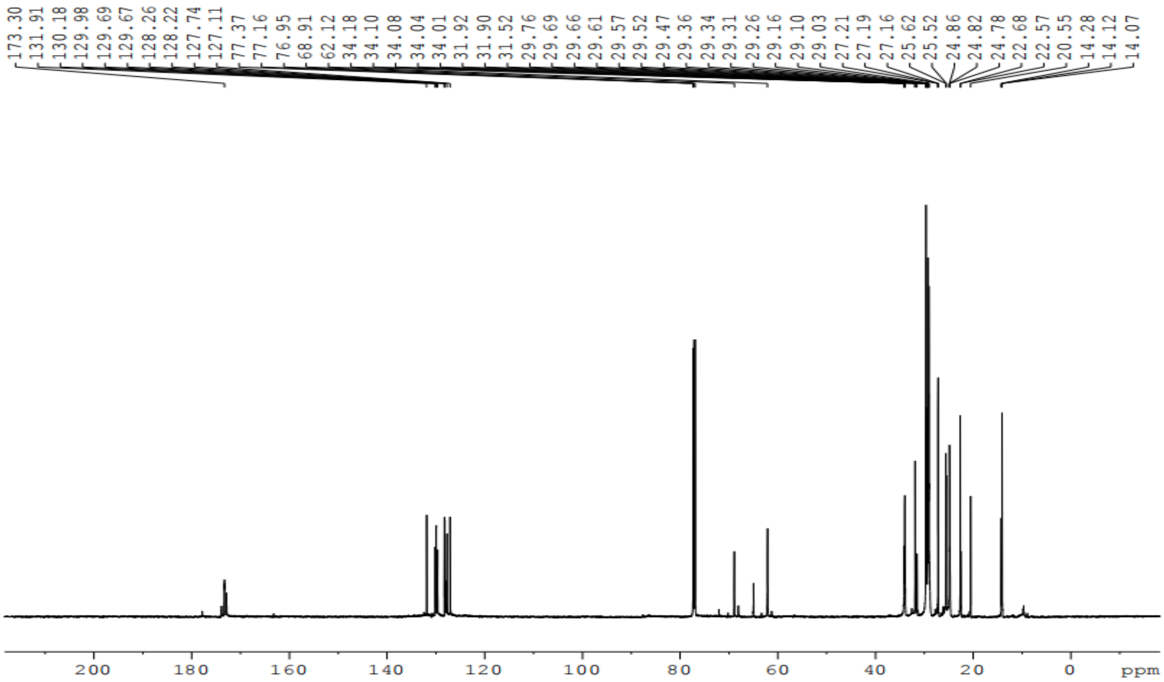

Figure 3. Carbon-13 nuclear magnetic resonance (13C NMR) of Castor oil (CO).

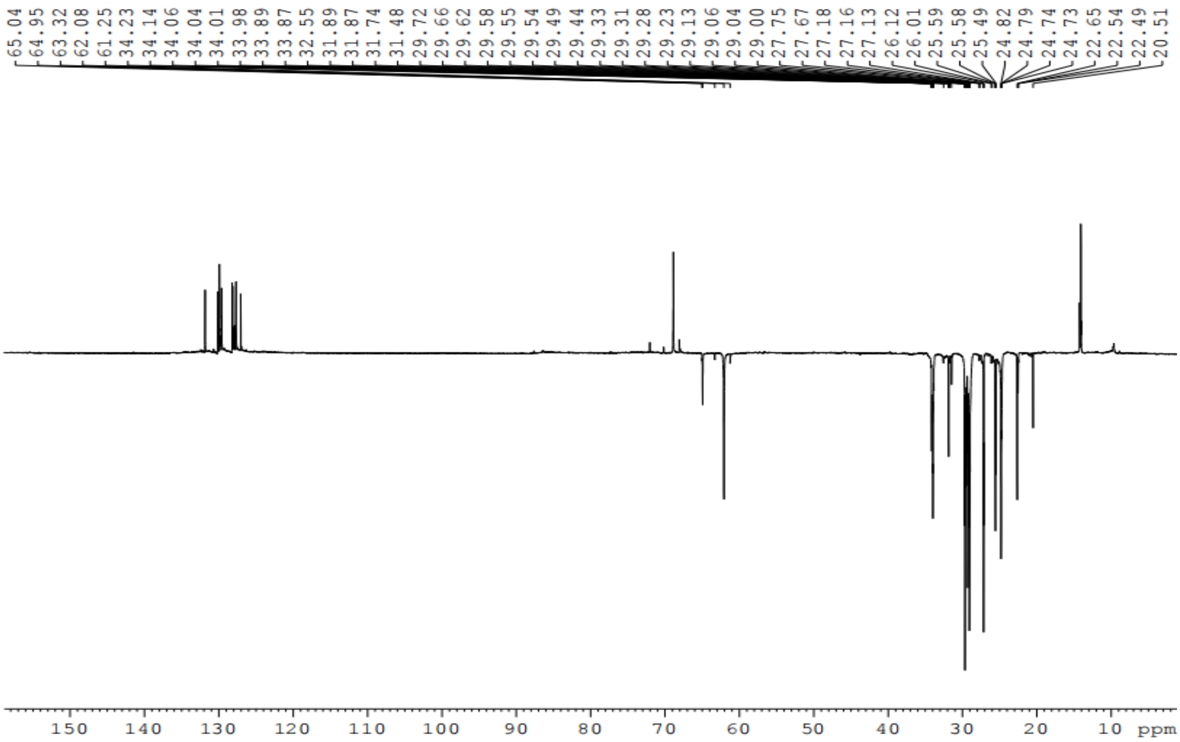

Figure 4. Distortionless enhancement by polarization transfer (DEPT-135) of castor oil (CO).

^{13}C NMR analysis showed peaks from δ_C 127.11 to 131.91 ppm, indicating unsaturated carbon in the oil. Similarly, peaks in the δ_C 76.94–77.37, 13.92–14.28, and 20–34.30 ppm ranges are due to deuterated chloroform, the terminal methyl carbon, and the methylene carbon of the long carbon chain, respectively, in the oil. The presence of a methylene group bonded to an electronegative atom, such as oxygen in castor oil, is indicated by a signal at δ_C 62.12–66.91 ppm, confirming the oil's status as an ester.

DEPT-135 analysis showed positive (up), negative (down), and positive (up) signals, confirming the presence of CH (methine), CH_2 (methylene), and CH_3 (methyl) groups, respectively, in the castor oil (**Figure 4**). The negative spectrum at δ_C 61.25–65.04 ppm indicates the glycerol backbone in castor oil. In addition, a positive signal at δ_C 68.09–72.05 ppm supports the presence of a triglyceride in the oil.

Hence, the castor oil used was found to be composed of triglycerides containing compounds with unsaturated carbon-carbon bonds.

From FTIR analysis, it was found that the castor oil exhibited the stretching vibration of the carboxyl group, indicated by the peaks in the 1680–1750 cm^{-1} region. This finding supports the presence of ester fatty acids [30] but not ricinoleic acid in this castor oil. Generally, the main constituent of castor oil is ricinoleic acid, having an -OH group [31,32]. Also, there was no impurity such as water [33]. The FTIR peaks of castor oil and castor boehmite nanofluid were similar to each other, as depicted in **Figure 5.** This can be attributed to the very small amount of B-NPs present in the oil. This small amount of NPs exhibits a feeble vibrational signal, whereas the vegetable oil background exhibits a high absorption band. 33>31, 31>33

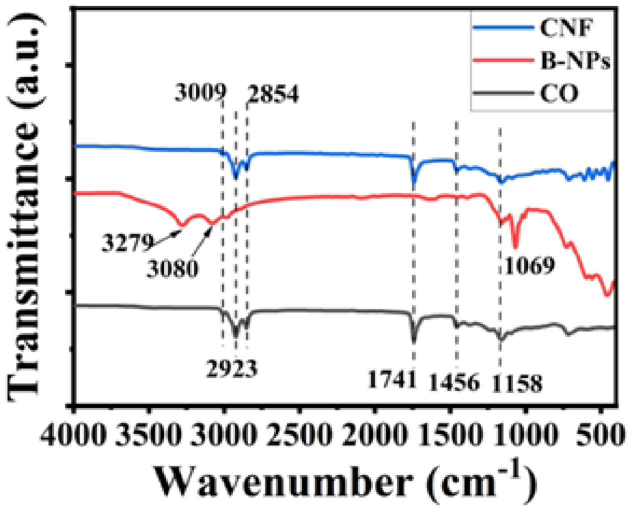

Figure 5. FTIR spectra of CO, B-NPs and its nanofluid, the CNF.

Additionally, there is no substantial interaction between the oil and the NPs. Therefore, the functional group remains unchanged, which confirms that the oil and the NPs interact only physically. This result is consistent with previous reports. For example, jatropha oil and its nanofluid had similar peaks [24]. No new peak was formed during the preparation of the nanofluid of thermal oil (hybrid NF) [34].

From thermogravimetric analysis (TGA) of castor oil (CO), the mass loss step was initiated significantly from 284.4 ℃ and ended at 461.3 ℃, leaving a final residue of 5.6%. The primary process that contributes to mass loss is the volatilization or decomposition of triglycerides with an increase in temperature.

The mass loss of the first step decreased with degradation time, and the mass loss of the second step increased, indicating the formation of higher molecular weight compounds that decomposed at higher temperatures. As the temperature rises further, there is no discernible mass loss, and the TG curve eventually becomes nearly flat, as shown in **Figure 6.**

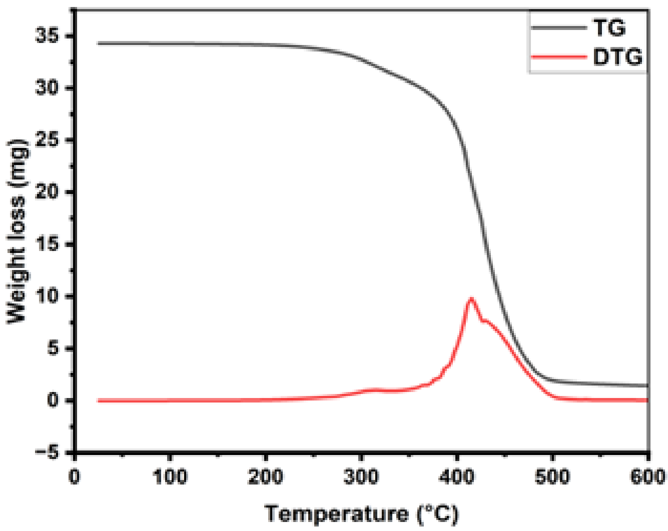

Figure 6. TG and DTG curves of castor oil (CO).

Accordingly, the derivative thermogravimetric analysis (DTG) curve shows a bimodal shape throughout the entire procedure, with a maximum mass loss of 9.61 mg/min at 418 ℃. The bimodal shape indicated that it was found to decompose in two steps. The first step may be due to the decomposition of the side-chain fatty acid of the triglyceride, and the second step is due to the breaking of its C-C-C skeleton. The pyrolysis of fatty acids occurs through C-C and C=O bond breaking by β-scission reaction, which may be due to deoxygenation of the C-C bond breaking to convert into hydrocarbon radicals, as well as deoxygenation of the short-chain molecule produced from the C-C bond breaking of the hydrocarbon chain [35].

3.3. Characterization of castor nanofluid (CNF)

In this study, the prepared CNF was characterized by investigating the stability test, K.V., V.I., pour point, and functional groups.

The stability of the nanofluid was studied by both visual (sedimentation) and zeta potential tests. The visual test, performed for up to 3 months, showed no sedimentation, indicating good stability. The zeta potential refers to the potential variation across solid-liquid phase boundaries. A higher value of zeta potential indicates higher stability. The zeta potential ranging from ±30 to ±60 mV and greater than ±60 mV indicates good and superior stability of the nanofluid, respectively [36-38].

From the zeta potential study, its value for the castor nanofluid was found to be −34.7 mV (**Figure 7a**), with a hydrodynamic size of 129.1 nm for B-NPs (**Figure 7b**), confirming its good stability. This is due to the stronger repulsive force among the NPs, which is responsible for forming a stable colloid and ensuring its long-term performance as a nanolubricant. In the case of jatropha nanofluid (JNF), the zeta potential of 27.3 mV indicated moderate stability and was beneficial only for short-term performance [24]. Hence, the castor nanofluid was found to be more stable than the jatropha nanofluid containing the same quantity of B-NPs. Hence, the effect of the NPs on the stability of the nanofluid is also observed in its K.V.

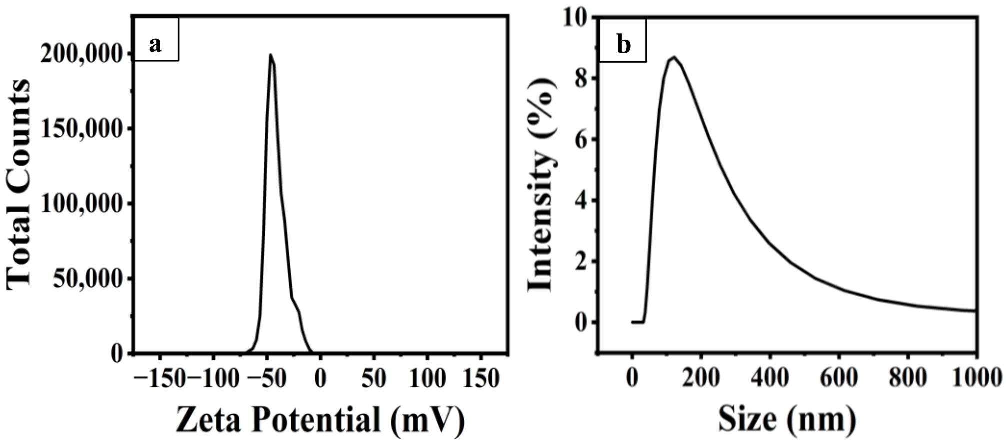

Figure 7. (**a**) Apparent zeta potential of the CNF and (**b**) hydrodynamic size of B-NPs in CNF.

From the K.V. study (see **Figure 8**), the nanofluid had higher values (76.96 ± 0.25, 38.34 ± 0.15, 20.09 ± 0.02, and 14.07 ± 0.02 cSt at 40 ± 0.5 ℃, 60 ± 0.5 ℃, 80 ± 0.5 ℃, and 100 ± 0.5 ℃ respectively) than that of neat oil (49.80 ± 0.23, 25.38 ± 0.11, 14.76 ± 0.05, and 10.41 ± 0.02 cSt) under similar temperatures, as presented in a bar diagram, **Figure 8a,b**. The formation of clusters, Brownian motion, and the interaction between the NPs and the fluid, which tends to resist the flow property, were the causes of the greater $K.V.$ values [39,40] of nanofluid.

The $K.V.$ decreased with temperature, following the model of the formula proposed by Arrhenius: $\eta(T) = \eta_o e^{-AE_a/T} + C$, where η_o is the viscosity at 0 ℃, E_a is the activation energy, A is a constant, which has the dimension of the inverse of Boltzmann's constant and C is a residual viscosity offset. The activation energy is an important parameter to understand the flowing nature of the fluid. It refers to the minimum energy possessed by the molecules to surpass the intermolecular forces and pass over one another [41,42]. In the case of oil, as the oil's temperature increased, its molecular kinetic energy also increased. As its molecular kinetic energy increased, more molecular collisions occurred, decreasing the intermolecular interaction between them. As a result, flow resistance decreases with increasing temperature. Similarly, as the temperature rose in a nanofluid, the molecular vibration of NPs increased as well. It impacted the formation of microstructure by reducing the nearest-neighbor contact, which led to a drop in the viscosity [43,44].

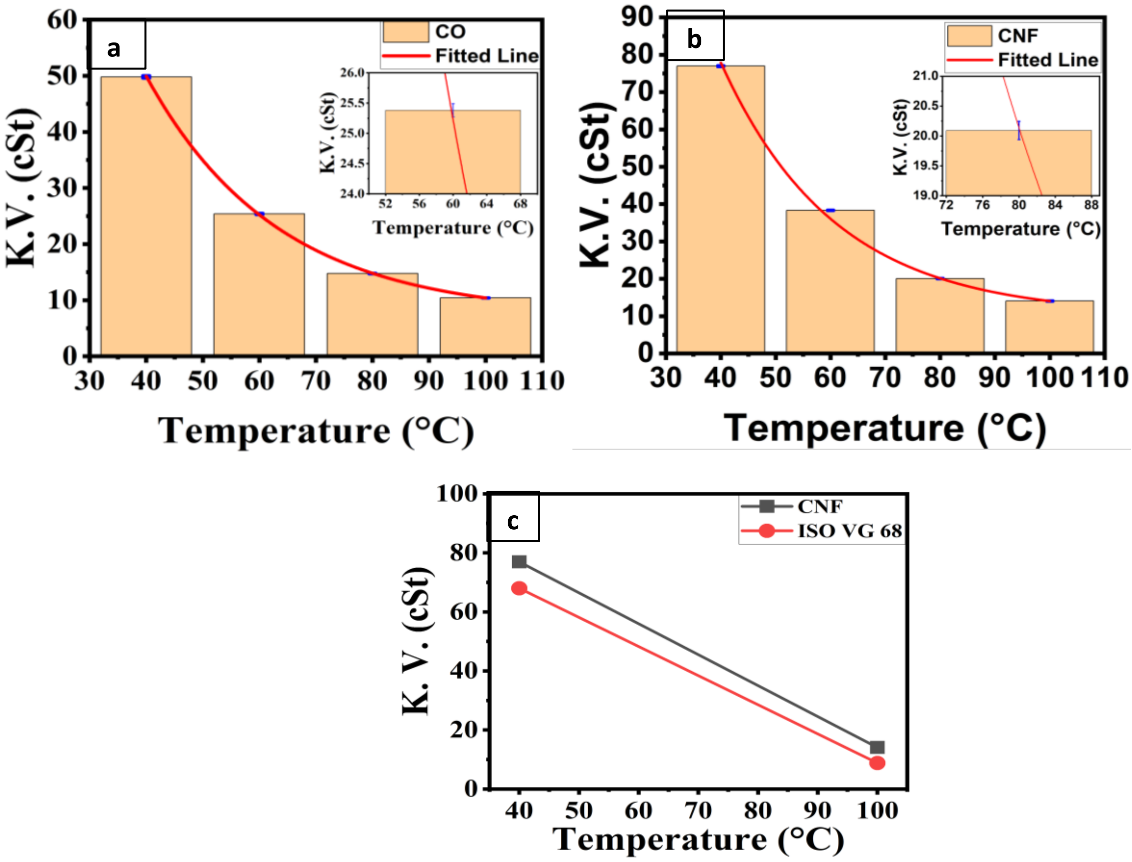

Figure 8. K.V. of (**a**) CO and (**b**) CNF at different temperatures, (**c**) comparison of K.V. of CNF and ISO VG 68 as indicated; a magnified error bar has been presented in (**a** and **b**) for clarity of understanding the statistical essence of the measurement.

When the thermal energy reaches the activation energy, the molecular vibration becomes maximum and acquires the saturation value beyond this temperature, which illustrates the smaller difference in $K.V.$ at higher temperatures that was observed in this work.

The $K.V.$ of the nanofluid was higher than that of castor oil at similar temperatures, which means that the K.V. was large (76.96 ± 0.25 cSt) at a lower temperature (40 ±0.5 ℃) and small (14.08 ±0.02 cSt) at a higher temperature (100 ± 0.5 ℃). The difference in $K.V.$ of nanofluid was large (27.16 ± 0.02 cSt) at low temperature (40 ±0.5 ℃) and small (3.66 cSt) at a higher temperature (100 ±0.5 ℃). The lower difference in $K.V.$ of CO and CNF at higher temperatures is due to an increase in Brownian motion, the break of clusters, and the weak particle-particle and particle-fluid interaction in nanofluid [39,40]. Pourpasha et al. (2020) also reported that the Brownian movement of nanoadditives in the pure lubricant is enhanced with temperature. Consequently, increasing the nanoadditive rate reduces the intermolecular forces between the lubricant and the nanoadditive's surface [44]. The relation of Brownian motion with temperature is given by the Einstein-Stokes equation: $x = \sqrt{\frac{2kTt}{3\pi\alpha\eta}}$ where a = diameter of particles, k = Boltzmann constant, η = viscosity, T = temperature, t = time, and x = distance [45,46]. As the temperature and molecular energy rise, the fluid's intermolecular forces diminish, increasing the intermolecular distance. Consequently, raising the temperature reduces the viscosity of nanofluids [45]. Zeinali Heris et al. (2015) also supported that Brownian motion increases with rising temperature [46].

The difference in K.V. after blending the NPs exhibited an exponential nature with temperature, following the Arrhenius equation. It is attributed to the higher molecular vibration of the added NPs present in the nanofluid [42]. The nature of the K.V. of castor nanofluid was similar to that of jatropha nanofluid [24]. The difference in K.V. of different vegetable oils at the same temperature depends on the fatty acid composition, the functional group present in the fatty acid, and the molecular weight of the oils [47].

It is noteworthy that only a small variation in K. V. values under similar experimental conditions was observed, confirming the good repeatability of experimental data. The reproducibility of K. V. of the nanofluid at 40, 60, 80, and 100 ℃, in terms of relative standard deviation, was 0.32%, 0.39%, 0.76%, and 1%. The observed low relative standard deviation also indicates the outstanding repeatability of the measurements.

Figure 8c illustrates that the K. V. value of the nanofluid is found to be 76.96 ± 0.25 cSt and 14.08 ± 0.02 cSt, at 40 ℃ and 100 ℃, respectively, while that of the mineral lubricant (as per International Organization for Standardization, Viscosity Grade 68; ISO VG 68) at the same temperatures has been reported as 68 cSt and 8.8 cSt, respectively [48]. The result of the KV obtained in this work is comparable with that reported for ISO VG 68. The ISO VG 68 must have 68 cSt K.V. at 40 ± 0.5 ℃. However, the minimum and maximum K.V. values of ISO VG 68 measured according to ASTM 445 vary from 61.2 to 74.8 cSt under the same temperature conditions [48]. Also, according to the National Fluid Power Association (NFPA) Recommended Practice, the allowable operating viscosity for the majority of pumps and motors should be between 13 and 860 mm^2/s [49], which supports the notion that the prepared nanofluid can be utilized in hydraulic systems.

The viscosity index (V.I.), a crucial lubricity property of the oil, was measured for the samples using ASTM D2270 and calculated using the formula: $.I. = \frac{(L-U)100}{(L-H)}$, where L = K.V. of fluids having a viscosity index 0 at 40 ℃, H = K.V. of fluids having a viscosity index 100 at 40 ℃ and U = K.V. of fluid at 40 ℃ [45,50].

As shown in **Figure 9a**, the nanofluid's V.I. was higher than that of the mineral oil-based lubricant. The higher V.I. of the nanofluid resulted from its composition of triglycerides (vegetable oil) and NPs, which are more stable than the mineral-based ISO VG 68, composed of hydrocarbons. A lower V.I. indicates lower viscosity stability with temperature [51].

In contrast, a higher V.I. indicates less viscosity change across temperatures [52,53]. A nanofluid with a high V.I. can help prevent excessive thickening [54]. Hence, the nanofluid prepared from castor oil, which has a higher viscosity index, is biodegradable and environmentally friendly and may be an excellent base stock for a green lubricant in place of ISO VG 68 (mineral lubricant). Furthermore, the nanofluid may serve as a high-performance lubricant.

The pour point is the lowest temperature at which the fluid stops flowing [55]. The pour point of the castor oil was found to be −3 ± 3 ℃, which dropped to −2 ± 3 ℃

in the nanofluid, which was only one degree higher than the oil. In other words, there was no significant change in the pour point of the nanofluid. This observation is consistent with the results reported by Karthikeyan et al., who investigated the castor oil-based nanofluid using molybdenum sulphide (MoS2) as the additive [56].

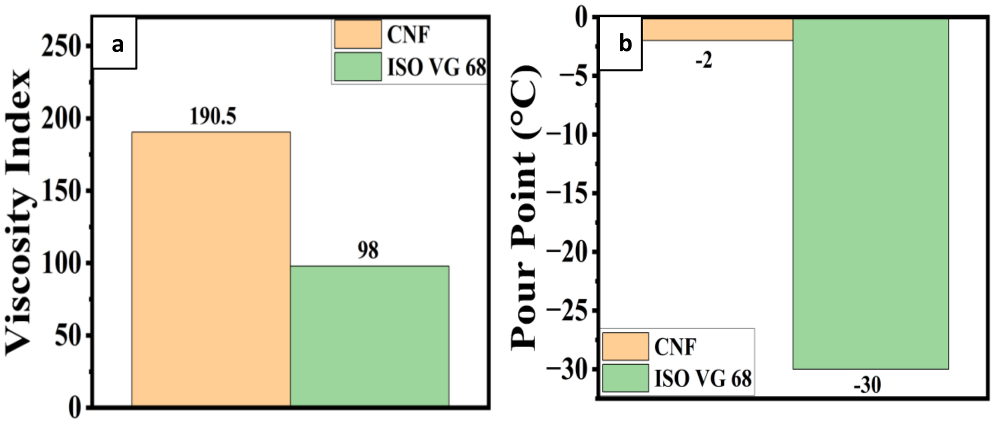

Figure 9. (**a**) Viscosity index of CNF and ISO VG 68, (**b**) Pour point of CNF and ISO VG 68 as indicated.

When comparing the pour point of the prepared nanofluid with that of ISO VG 68 mineral hydraulic oil, the nanofluid's pour point was relatively higher (−2 ℃) than that of ISO VG 68 mineral hydraulic oil (−30 ℃), as shown in **Figure 9b,** and could be improved by the addition of pour point depressants. In other words, we can say that the nanofluid had comparatively poor cold flow behavior and was not very good for cold climates. Hence, the nanofluid can be used as a green hydraulic fluid in warm places.

4. Conclusion

The present study has sought to improve the lubricating properties of castor oil by dispersing B-NPs and manipulating the oil's flow behavior, as measured by viscosity. Before blending, B-NPs were characterized by X-ray diffraction (XRD) and transmission electron microscopy (TEM). XRD and TEM analyses revealed a crystallite size of 8.3 nm and a platelet-like structure with a diameter of 8.3 nm. The castor oil-based nanofluid was prepared by blending 0.1 wt.-% of polycrystalline and platelet-like textured B-NPs.

The kinematic viscosity of castor oil was found to increase well with the addition of a small amount of the NPs (0.1 wt.-% in the present case), which decreased as expected progressively at elevated temperature.

The zeta potential of the nanofluid was −34.7 mV, indicating good stability and suitability for long-term performance. Thus, the NPs have been demonstrated as being excellent viscosity modifiers.

The results so far obtained have demonstrated the castor oil-based nanofluid's suitability as a potential eco-friendly bio-based lubricant as an alternative to the corresponding petroleum-based fluids. The notion of the nanofluid being recognized as a green lubricant for warm environments is supported by its superior viscosity index, higher pour point, and comparable kinematic viscosity to mineral lubricants.

More experiments on the effect of the NPs concentration and surfactants on the viscosity and tribological properties are ongoing, and the results will be reserved for publication in the near future.

Author contributions: SKJ: Manuscript drafting, original manuscript preparation, formal analysis, DKC: Co-drafting, data analysis, MAM: Zeta potential analysis, MSI: NMR analysis, MAG: TGA analysis, ANA: TGA analysis, results interpretation, RPD: Validation, formal analysis, supervision, resource, editing, SPA: Validation, formal analysis, supervision, SMH: Formal analysis, validation, supervision, RA: Conceptualization, co-drafting, resources, supervision, manuscript editing.

Acknowledgments: SKJ is very thankful to Nepal Oil Corporation Limited for providing the study leave and laboratory facilities to conduct a part of the research project. The authors are grateful to the International Science Program at Uppsala University, Sweden, for providing a fellowship to SKJ, enabling her research stay at the Material Science Division of the Atomic Energy Centre in Dhaka, Bangladesh, under program BAN:02/2; and the Bangladesh Council of Scientific and Industrial Research, Bangladesh (BCSIR) for supporting with NMR results. We thank Dr. Sven Henning, Fraunhofer Institute, and Prof. Goerg H. Michler, Halle, Germany, for his support in arranging the boehmite nanoparticles.

Conflict of interest: The authors declare that they have no conflicts of interest. All the authors have read and approved the manuscript.

References

1. Anderson KJ. A History of Lubricants. MRS Bull. 1991; 16(10): 69–69. doi: 10.1557/S0883769400055895
2. Spikes H. The History and Mechanisms of ZDDP. Tribol. Lett. 2004; 17(3): 469–489. doi: 10.1023/B:TRIL.0000044495.26882.b5
3. Zainal NA, Zulkifli NWM, Gulzar M, Masjuki HH. A Review on the Chemistry, Production, and Technological Potential of Bio-Based Lubricants. Renew. Sustain. Energy Rev. 2018; 82: 80–102. doi: 10.1016/j.rser.2017.09.004
4. Sharma P, Sidhu BS, Sharma J. Investigation of Effects of Nanofluids on Turning of AISI D2 Steel Using Minimum Quantity Lubrication. J. Clean. Prod. 2015; 108: 72–79. doi: 10.1016/j.jclepro.2015.07.122
5. Singh AK, Kumar A, Sharma V, Kala P. Sustainable Techniques in Grinding: State of the Art Review. J. Clean. Prod. 2020; 269: 121876. doi: 10.1016/j.jclepro.2020.121876
6. Lee K, Hwang Y, Cheong S, et al. Understanding the Role of Nanoparticles in Nano-Oil Lubrication. Tribol. Lett. 2009; 35: 127–131. doi: 10.1007/s11249-009-9441-7
7. Maurya U, Vasu V. Boehmite Nanoparticles for Potential Enhancement of Tribological Performance of Lubricants. Wear. 2022; 498: 204311. doi: 10.1016/j.wear.2022.204311
8. Choi SU, Eastman JA. Enhancing Thermal Conductivity of Fluids with Nanoparticles. Argonne, IL: Argonne National Lab.(ANL); 1995. doi: 10.1115/IMECE1995-0926
9. Eastman JA, Choi SUS, Li S, Yu W, Thompson LJ. Anomalously Increased Effective Thermal Conductivities of Ethylene Glycol-Based Nanofluids Containing Copper Nanoparticles. Appl. Phys. Lett. 2001; 78(6): 718–720. doi: 10.1063/1.1341218
10. Saidur R, Leong KY, Mohammed HA. A Review on Applications and Challenges of Nanofluids. Renew. Sustain. Energy Rev. 2011; 15(3): 1646–1668. doi: 10.1016/j.rser.2010.11.035
11. Sarkar J, Ghosh P, Adil A. A Review on Hybrid Nanofluids: Recent Research, Development and Applications. Renew. Sustain. Energy Rev. 2015; 43: 164–177. doi: 10.1016/j.rser.2014.11.023
12. Solangi KH, Kazi SN, Luhur MR, et al. A Comprehensive Review of Thermo-Physical Properties and Convective Heat Transfer to Nanofluids. Energy. 2015; 89: 1065–1086. doi: 10.1016/j.energy.2015.06.105

13. Suhaib B, Awan SE, Awais M, et al. Peristaltic rheology of nanomaterial in a porous channel under thermal radiation and variable heat source: An artificial neural network framework. Chaos, Solitons & Fractals. 2026; 203: 117638. doi: 10.1016/j.chaos.2026.117638
14. Wang Y, Wan Z, Lu L, Zhang Z, Tang Y. Friction and Wear Mechanisms of Castor Oil with Addition of Hexagonal Boron Nitride Nanoparticles. Tribol. Int. 2018; 124: 10–22. doi: 10.1016/j.triboint.2018.03.035
15. Gupta RN, AP H. Tribological Study of Castor Oil with Surface-Modified CuO Nanoparticles in Boundary Lubrication. Ind. Lubr. Tribol. 2018; 70(4): 700–710. doi: 10.1108/ILT-02-2017-0030
16. Gupta RN, Harsha A. Antiwear and Extreme Pressure Performance of Castor Oil with Nano-Additives. Proc. Inst. Mech. Eng. Part J J. Eng. Tribol. 2018; 232(9): 1055–1067. doi: 10.1177/1350650117739159
17. Bhaumik S, Maggirwar R, Datta S, Pathak SD. Analyses of Anti-Wear and Extreme Pressure Properties of Castor Oil with Zinc Oxide Nano Friction Modifiers. Appl. Surf. Sci. 2018; 449: 277–286. doi: 10.1016/j.apsusc.2017.12.131
18. Singh Y, Chaudhary V, Pal V. Friction and Wear Characteristics of the Castor Oil with TiO_2 as an Additive. Mater. Today Proc. 2020; 26: 2972–2976. doi: 10.1016/j.matpr.2020.02.612
19. Mart ń-Alfonso JE, Mart ń-Alfonso MJ, Franco JM. Tunable Rheological-Tribological Performance of "Green" Gel-like Dispersions Based on Sepiolite and Castor Oil for Lubricant Applications. Appl. Clay Sci. 2020; 192: 105632. doi: 10.1016/j.clay.2020.105632
20. Vora V, Sharma RK, Bharambe DP. Investigation of Rheological and Thermal Conductivity Properties of Castor Oil Nanofluids Containing Graphene Nanoplatelets. Int. J. Thermophys. 2023; 44(10): 155. doi: 10.1007/s10765-023-03264-5
21. Yepuri V, Ramachandramurthy P. Impact of Sol-Gel Synthesized α-Aluminium Oxide Nanoparticles for the Enhancement of Transformer Oil Insulation Properties. Kuwait J. Sci. 2025; 52(1): 100331. doi: 10.1016/j.kjs.2024.100331
22. Sun T, Zhuo Q, Chen Y, Wu Z. Synthesis of Boehmite and Its Effect on Flame Retardancy of Epoxy Resin. High Perform. Polym. 2015; 27(1): 100–104. doi: 10.1177/0954008314540312
23. Mohammadi M, Khodamorady M, Tahmasbi B, Bahrami K, Ghorbani-Choghamarani A. Boehmite Nanoparticles as Versatile Support for Organic–Inorganic Hybrid Materials: Synthesis, Functionalization, and Applications in Eco-Friendly Catalysis. J. Ind. Eng. Chem. 2021; 97: 1–78. doi: 10.1016/j.jiec.2021.02.001
24. Joshi SK, Chaudhary DK, Mamun MA, et al. Boehmite Nanoparticle-Enhanced Jatropha Oil Nanofluid: Synthesis, Stability, and Viscosity Analysis. J. Nepal Chem. Soc. 2025; 45(2): 125–134. doi: 10.3126/jncs.v45i2.83055
25. Ogata F, Kawasaki N, Nakamura T, Tanada S. Removal of Arsenious Ion by Calcined Aluminum Oxyhydroxide (Boehmite). J. Colloid Interface Sci. 2006; 300(1): 88–93. doi: 10.1016/j.jcis.2006.03.026
26. Lepot N, Van Bael MK, Van Den Rul H, et al. Synthesis of Platelet-Shaped Boehmite and γ-Alumina Nanoparticles via an Aqueous Route. Ceram. Int. 2008; 34(8): 1971–1974. doi: 10.1016/j.ceramint.2007.07.022
27. Brostow W, Datashvili T. Chemical Modification and Characterization of Boehmite Particles. Chem. Chem. Technol. 2008; 2(1): 27–32. doi: 10.23939/chcht02.01.027
28. Roy S, Maity A, Mandal P, et al. Effects of Various Morphologies on the Optical and Electrical Properties of Boehmite Nanostructures. CrystEngComm. 2018; 20(40): 6338–6350. doi: 10.1039/C8CE01171K
29. Sudheer N, Rouchon V, Ihiawakrim D, et al. Investigating the Crystallite Morphologies and Aggregation in Boehmite Powders: A Combined Analysis of Two- and Three-Dimensional Electron Microscopy with X-Ray Diffraction. Sci. Technol. Energy Transit. 2024; 79: 84. doi: 10.2516/stet/2024050
30. Tariq M, Qureshi AK, Imran M, et al. Biodiesel—a Transesterified Product of Non-Edible Castor Oil. Rev. Roum. Chim. 2020; 64(12): 1027–1036. doi: 10.33224/rrch/2019.64.12.02
31. Nitbani FO, Tjitda PJP, Detha AIR. Preparation of Ricinoleic Acid from Castor Oil: A Review. J Oleo Sci. 2022; 71(6): 781–793. doi: 10.5650/jos.ess21226
32. Chauke NP, Mukaya HE, Nkazi DB. Chemical Modifications of Castor Oil: A Review. Sci. Prog. 2019; 102(3): 199–217. doi: 10.1177/0036850419859118
33. Jayagobi M, Alpandi AH, Husin H. Characterization of Malaysian Jatropha Seed Oil using FTIR and GCMS. Platf. J. Eng. 2021; 5(4): 23. doi: 10.61762/pajevol5iss4art15266
34. Ahmed A, Ilyas SU. Rheological Profile of Surfactant-Free Non-Newtonian MWCNT-Oil Hybrid Nanofluids with Carbon Nanofiber Additives. ACS Omega. 2025; 10(29): 31331–31347. doi: 10.1021/acsomega.4c10749
35. Li H, Niu S, Lu C. Pyrolysis Characteristics of Castor Oil through Thermogravimetric Coupled with Fourier Transform Infrared Spectroscopy. Procedia Eng. 2017; 205: 3705–3710. doi: 10.1016/j.proeng.2017.10.292

36. Kumar KR, Shaik AH. Synthesis, Thermophysical Characterization and Thermal Performance Analysis of Novel Cu-MXene Hybrid Nanofluids for Efficient Coolant Applications. RSC Adv. 2023; 13(42): 29536–29560. doi: 10.1039/D3RA05429B
37. Pawar NR, Pawar M, Chavhan RD, Chimankar OP. Synthesis and Spectroscopic Characterization of Boehmite Nanoparticles and Its Thermodynamic Study. J. Pure Appl. 2020; 42: 59–65. http://ultrasonicsindia.org/JPAU-42-3-2020.pdf#page=5
38. Kong L, Sun J, Bao Y. Preparation, Characterization and Tribological Mechanism of Nanofluids. RSC Adv. 2017; 7(21): 12599–12609. doi: 10.1039/C6RA28243A
39. Nurdin I, Yaacob II, Johan MR. Enhancement of Thermal Conductivity and Kinematic Viscosity in Magnetically Controllable Maghemite (γ-Fe_2O_3) Nanofluids. Exp. Therm. Fluid Sci. 2016; 77: 265–271. doi: 10.1016/j.expthermflusci.2016.05.002
40. Babar H, Sajid M, Ali H. Viscosity of Hybrid Nanofluids: A Critical Review. Therm. Sci. 2019; 23(3 Part B): 1713–1754. doi: 10.2298/TSCI181128015B
41. Ike E. The Study of Viscosity-Temperature Dependence and Activation Energy for Palm Oil and Soybean Oil. Glob. J. Pure Appl. Sci. 2019; 25(2): 209–217. doi: 10.4314/gjpas.v25i2.11
42. Ike E. Arrhenius-Type Relationship of Viscosity as a Function of Temperature for Mustard and Cotton Seed Oils. Niger. Ann. PURE Appl. Sci. 2020; 3(3b): 144–155. doi: 10.46912/napas.205
43. Nabeel Rashin M, Hemalatha J. Synthesis and Viscosity Studies of Novel Ecofriendly ZnO–Coconut Oil Nanofluid. Exp. Therm. Fluid Sci. 2013; 51: 312–318. doi: 10.1016/j.expthermflusci.2013.08.014
44. Nabeel Rashin M, Hemalatha J. Viscosity Studies on Novel Copper Oxide–Coconut Oil Nanofluid. Exp. Therm. Fluid Sci. 2013; 48: 67–72. doi: 10.1016/j.expthermflusci.2013.02.009
45. Pourpasha H, Heris SZ, Mahian O, Wongwises S. The effect of multi-wall carbon nanotubes/turbine meter oil nanofluid concentration on the thermophysical properties of lubricants. Powder technology. 2020; 367: 133–142. doi: 10.1016/j.powtec.2020.03.046
46. Zeinali Heris S, Razbani MA, Estellé P, Mahian O. Rheological behavior of zinc-oxide nanolubricants. Journal of Dispersion Science and Technology. 2015; 36(8): 1073–1079. doi: 10.1080/01932691.2014.935455
47. Geller DP, Goodrum JW. Rheology of Vegetable Oil Analogs and Triglycerides. J. Am. Oil Chem. Soc. 2000; 77(2): 111–114. doi: 10.1007/s11746-000-0018-4
48. Pitakjakpipop P, Khudkham T, Anutrasakda W, et al. Valorization of Palm Fatty Acid Distillate to Oleochemical Estolide Esters for Use as Biolubricant Base Oils. Fuel. 2026; 407: 137253. doi: 10.1016/j.fuel.2025.137253
49. Herzog SN, Placek DG, Simko RP, Neveu CD. Predicting the Pump Efficiency of Hydraulic Fluids to Maximize System Performance. 2002; 2002-01-1430. doi: 10.4271/2002-01-1430
50. Mousavi SB, Zeinali Heris S, Estellé P. Experimental comparison between ZnO and MoS_2 nanoparticles as additives on performance of diesel oil-based nano lubricant. Scientific reports. 2020; 10(1): 5813. doi: 10.1038/s41598-020-62830-1
51. He L, Su S, Zhao Y, et al. Intrinsic relationship between viscosity, viscosity index, and molecular structure of isoalkanes. J Mol Model. 2023; 29: 101. doi: 10.1007/s00894-023-05494-8
52. Wang H, Wang Y, Wen P, et al. Low-Viscosity Oligoether Esters (OEEs) as High-Efficiency Lubricating Oils: Insight on Their Structure–Lubricity Relationship. Friction. 2024; 12(6): 1133–1153. doi: 10.1007/s40544-023-0765-3
53. Naddaf A, Zeinali Heris S. Density and rheological properties of different nanofluids based on diesel oil at different mass concentrations. Journal of Thermal Analysis and Calorimetry. 2019; 135(2): 1229–1242. doi: 10.1007/s10973-018-7519-3
54. Kotia A, Sharma RK, Sharma P, et al. Rheological Analysis on Joannesia Princeps Oil for Sustainable Bio-Lubricant in Electric Vehicle Application. IOP Conf. Ser. Mater. Sci. Eng. 2021; 1116(1): 012015. doi: 10.1088/1757-899X/1116/1/012015
55. Musa GA, Adawara SN, Isa AS, et al. Production and Characterization of Biolubricants from Neem Seed Oil. 2026; 2: 59–69. doi: 10.22034/jchemtech.2026.571895.1033
56. Karthikeyan KMB, Vijayanand J, Arun K, Seshagiri Rao V. Thermophysical and Wear Properties of Eco-Friendly Nano Lubricants. Mater. Today Proc. 2021; 39: 285–291. doi: 10.1016/j.matpr.2020.07.128